Age-related effects on cortical thickness patterns of the Rhesus monkey brain

Bang-Bon Koo[a,b], Steven P. Schettler[a], Donna E. Murray[a], Jong-Min Lee[c], Ronald J. Killiany[a], Douglas L. Rosene[a,e], Dae-Shik Kim[a,b,d], Itamar Ronen[a,b,f,*]

[a] Department of Anatomy and Neurobiology, Boston University School of Medicine, Boston, MA, USA
[b] Center for Biomedical Imaging, Boston University School of Medicine, Boston, MA, USA
[c] Department of Biomedical Engineering, Hanyang University, Seoul, South Korea
[d] Department of Electrical Engineering, Korea Advanced Institute of Science and Technology, Daejeon, South Korea
[e] Yerkes National Primate Research Center, Emory University, Atlanta, GA, USA
[f] Department of Radiology, Leiden University Medical Center, Leiden, The Netherlands

Abstract

The Rhesus monkey is a useful model for examining age-related as well as other neurological and developmental effects on the brain, because of the extensive neuroanatomical homology to the human brain, the reduced occurrence of neurological diseases such as Alzheimer's disease, and the possibility of obtaining relevant behavioral data and post-mortem tissue for histological analyses. In this study, cortical thickness measurements based on a cortical surface modeling technique were applied for the first time to investigate cortical thickness patterns in the rhesus monkey brain, and were used to evaluate regional age related effects across a wide range of ages. Age related effects were observed in several cortical areas, in particular in the somato-sensory and motor cortices, where a robust negative correlation of cortical thickness with age was observed, similar to that found in humans. In contrast, results for monkeys compared with humans show significant interspecies differences in cortical thickness patterns in the frontal and the inferior temporal regions.
© 2012 Elsevier Inc. All rights reserved.

Keywords: Aging brain; Rhesus monkey; Gray matter; Cerebral cortex; Cortical surface modeling; Cortical thickness

1. Introduction

The Rhesus monkey (*Macaca mulatta*) model of normal aging is useful in the context of investigating age-related morphological changes in the human brain (Roth et al., 2004). The Rhesus monkey shows patterns of age-related cognitive decline that are similar to those expressed in humans (Herndon et al., 1997; Moss et al., 1988; Moss, et al., 1997), while being less affected by neurodegenerative diseases, such as Alzheimer's disease (Peters et al., 1998; Roth et al., 2004). The faster aging process of rhesus monkeys (Tigges et al., 1988), about three times faster compared with humans, offers distinct advantages for aging research, in addition to better control over health and other life-style factors that increase the variability of age effects in humans.

Several studies in humans suggest that normal aging strongly correlates with morphological alteration of cortical structures (Raz and Rodrigue, 2006; Raz et al., 2005). Although observed age-related trajectories of cortical characteristics need to be carefully interpreted due to the significant variability across studies, some relatively consistent patterns of age-related morphological changes have been observed. In recent as well as in some older large-scale studies, highly consistent decrease in cortical gray matter (GM) volume in old age was observed (Jernigan et al., 2001; Walhovd et al., 2009). Detailed analysis of regional morphometric age-related changes showed that these changes are often nonlinear, with some areas showing first increase in gray matter density and then decline, while other areas exhibited

* Corresponding author: Tel.: +31 71 526 5479.
  E-mail address: i.ronen@lumc.nl (I. Ronen).

an opposite trend (Sowell et al., 2003; Walhovd et al., 2009). Cerebral white matter (WM) volume was also often found to change with age, most recently in a study that found increase in WM volume until middle age, followed by a subsequent decrease (Walhovd et al., 2009).

Only a handful of studies used morphometric analysis of MRI data for aging research in nonhuman primates, despite its generally accepted usefulness as an animal model for aging studies. Most of the reports showed age-related decline in both subcortical structures, such as caudate nucleus and putamen volume, and global gray and/or white matter tissue volumes (Matochik et al., 2000; Wisco et al., 2008). One study based on regional voxel based analysis showed significant bilateral reductions in gray matter of the prefrontal and temporal pole region during aging in Rhesus monkeys (Alexander et al., 2008).

Overall characteristics of the cortex can be efficiently confirmed from a three-dimensional (3D) representation of the cortical surface and one particularly interesting feature is cortical thickness (Dale et al., 1999; Fischl and Dale, 2000; Kim et al., 2005; Lee et al., 2006). An increasingly growing body of work has suggested that cortical thickness as calculated from human MRI data correlates well with age. Most studies showed prominent age-related indications of cortical thinning in prefrontal, somato-sensory and motor cortex, while other regions, such as the temporal and para-hippocampal cortex, seemed to remain relatively unaffected (Salat et al., 2004). However, combining functional and behavioral measurements with cortical thickness measurements in humans revealed a rather complex picture of structural changes in aging. In one study, old subjects with high fluid abilities had significantly higher cortical thickness than old subjects with average fluid abilities and young subjects in several cortical regions, in particular in the posterior cingulated, and an overall analysis suggests a nonlinear change in overall cortical thickness that is different for the high- and average performers in the fluidity tests (Fjell et al., 2006). In another study, robust cortical thinning was detected in somato-sensory and motor cortices, but no correlation was found between cortical thickness of the older adults and a host of cognitive measures (Ziegler et al., 2008).

Although cortical surface modeling has been successfully applied to rhesus monkey brain, its application to morphometric studies in monkeys has been limited. The first study that applied cortical surface modeling to the rhesus monkey brain used this technique to define the morphometric correspondence between human and monkey visual areas (Van Essen et al., 2001). Another application focused on the visualization of functional maps (Vincent et al., 2007).

In this work, a cortical surface modeling technique is used for the first time to investigate cortical thickness patterns in the rhesus monkey brain, and focuses on providing initial observations obtained from cross-sectional investiga-

Table 1
Rhesus monkey population: subjects age and sex at time of scan

Subject no.	Sex	Age
1	M	6.1
2	M	6.3
3	M	7.2
4	M	8.4
5	F	11.4
6	F	14.1
7	F	15.2
8	F	15.2
9	F	15.9
10	F	16.1
11	F	16.9
12	F	17
13	F	17.6
14	F	18.5
15	M	20.2
16	F	20.6
17	M	24.4
18	M	26.5

tion of regional age-effects on cortical thickness in the rhesus monkey brain across a wide range of ages (6–27 years).

2. Methods

2.1. Subjects and imaging protocol

2.1.1. Animal subjects

A total of 18 Rhesus monkeys, ranging in age from 6.1 to 26.5 years old, were selected for this study. Table 1 specifies the age and sex of all monkeys that participated in this study. Selection criteria for monkeys to participate in this study excluded any animals exposed experimentally to neuroactive drugs, and animals with a history of any neurological symptoms. In addition, monkeys with chronic illness, any impairments of the immune system, any evidence of diabetes or defects in visual or motor functions that would limit behavioral testing were excluded from this study. All selected monkeys were also given an initial anatomical MRI scan to exclude any occult neurological problems.

2.1.2. Animal procedures

All experimental procedures were approved by the Institutional Animal Care and Use Committee (IACUC) of Boston University Medical Campus and conformed to National Institutes of Health (NIH) guidelines. For scanning, monkeys were anesthetized with an initial dose of ketamine, 10 mg kg^{-1} i.m. and xylazine, 0.05 mg kg^{-1} i.m. and brought to the scanner. In the scanner, animals were put in an MRI-compatible stereotactic head-holder specially designed to fit within the radiofrequency coil used for the experiment. Body temperature was measured before the experiment and immediately after the scan was over. An MRI-compatible pulse oximeter sensor supplied with the MRI scanner was positioned on the monkey's rear foot for continuous reading

of heart rate and oxygenation, and a respiration belt was positioned under the monkey's abdomen to monitor respiration rate. Ketamine boosters were provided as needed throughout the experiment to maintain a uniform level of anesthesia, typically once every 20–25 minutes.

2.1.3. MRI experiments

All experiments were performed on a whole body 3T MRI Philips Intera scanner (Philips Medical Systems, Best, the Netherlands). Radiofrequency (RF) coil used for this experiment was the 6-channel synergy receive-only head coil, while RF transmission was done through the quadrature body coil. The six channels in the head coil were combined in quadrature mode.

2.1.4. MRI scans

T_1-weighted images were acquired with a 3D-T_1-TFE sequence with the following parameters: TR/TE = 9 ms/6 ms, Intershot delay = 2,800 ms, TFE factor = 200, NEX = 6, for a data matrix of 256 × 256 × 140, FOV: 156 × 156 × 78 mm^3, yielding a resolution of 0.6 × 0.6 × 0.61 mm^3. Acquisition time was about 45 minutes.

2.2. Cortical surface modeling and cortical thickness

2.2.1. Cortical surface modeling

Cortical surface modeling technique consisted of several sequential image processing steps. First, intensity nonuniformities stemming from inhomogeneities in the radiofrequency field were corrected in all images (Sled et al., 1998). Subsequently, nonbrain tissue was eliminated using brain extraction algorithm (Smith 2002). Then, images were registered into a standard rhesus monkey average template (McLaren et al., 2009) (www.brainmap.wisc.edu/monkey. html) using affine transformation (Collins et al., 1994). GM, WM, and cerebrospinal fluid (CSF) regions were defined on spatially normalized MRI images using k-nearest neighbor classification method (Cocosco et al., 2003). Here, the rhesus monkey tissue prior templates were applied for precise tissue estimation (McLaren et al., 2009). Finally, cortical surface modeling for the rhesus monkey was performed using constrained Laplacian-based automated segmentation with proximities (CLASP) algorithm (Kim et al., 2005) in which the GM/WM interface is reconstructed by deforming a spherical polygon model to the white matter boundary. Because the cortical surface area of rhesus monkey brain (~11,000 mm^2) is significantly smaller than that of the human brain (~92,400 mm^2), the initial surface structure was set to have 5,000 vertices, whereas the number of vertices used in humans is typically set to about 40,000. The Laplacian field map was then generated between the WM boundary and the CSF skeleton. Using the Laplacian field map, WM/GM interface was smoothly expanded to model the GM/CSF interface. Finally, the GM/CSF and WM/GM interfaces were transformed from the template space to native subject space using the inverse affine transformation.

2.2.2. Cortical thickness calculation

A point-to-point correspondence between the two interfaces was automatically defined after final surface reconstruction and used to derive measures of cortical thickness at each of the 5,000 point-to-point vertices (Lerch and Evans, 2005). Reconstructed surfaces were then overlapped with 3D structural volume images to check whether the cortical surface representation fits well with the tissue boundaries shown in the structural image. The reconstruction of the surfaces and the resulting cortical thickness estimation for three of the data sets is shown in Figure 1.

Following the surface modeling for each subject, an average rhesus monkey surface was then reconstructed from vertex-by-vertex averaging of the middle surface between the GM/WM interface and the GM/CSF interface (Figure 2, abbreviations are given in Table 2). For proper local shape averaging, each subject's surface in the template space (before applying the inverse affine transformation) was used for averaging. The main purpose of the average surface construction was to provide a standard target brain surface for performing the cortical pattern matching algorithm (Lyttelton et al., 2007; Robbins et al., 2004). The cortical pattern matching technique used here defines one-to-one point correspondences between the average surface and individual surfaces based on sulcal-gyral feature matching. This procedure provides accurate matching of morphologically homologous cortical locations among participants on the basis of each individual's anatomy. Subsequently, each subject's surface information was then mapped onto the average surface template for group analyses.

2.3. Data analysis

For age-related group analysis, two age groups were defined as follows: a "young adults" group, which included monkeys between 6 and 15.2 years old (10.48 ± 3.98 year/o, n = 8, male: four/female: four), and an "old" group that comprised of monkeys older than 17.5 (21.3 ± 3.46 year/o, n = 6, male: three/female: three). It has been suggested that a strong correlation exists between sex and brain size in rhesus monkeys (Franklin et al., 2000). To minimize the possible influence of this correlation on our group analysis, we excluded the excess nonsex-matched female monkeys (Subjects 9–12 in Table 1) from this particular analysis.

2.4. Age-related effects on cortical thickness: mapping and statistical analysis

Age-related effects on cortical thickness were explored with both group and regression analyses. Mean cortical thickness in each group was mapped and assessed for qualitative assessment of overall patterns and differences between the groups. For quantitative analysis, mean value comparisons of cortical thickness in each lobe, as well as point-wise value comparisons were performed.
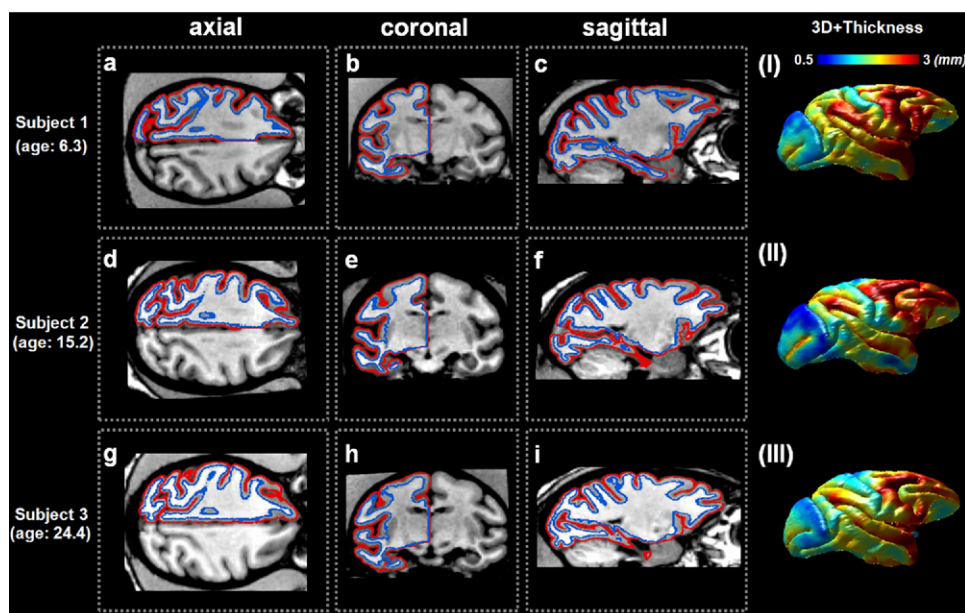
Fig. 1. Cortical surface modeling in three individual monkeys of different ages (a-c: age 6.3 years; d-f: age 15.2 years; g-i: age 24.4) viewed in axial, coronal and sagittal sections. Right hemisphere gray matter/csf and gray/white matter surface models are marked in red and blue lines, respectively. The rightmost column shows three-dimensional representation of the corresponding gray/csf surface model for each monkey brain overlaid with the corresponding cortical thickness map.

For lobe-wise analysis, the cortical surface was manually divided into eight different regions according to Styner et al. (Styner et al., 2007). Independent sample *t*-statistics was used to test the group differences. Linear regression was performed to evaluate age-related effects in the entire group of monkeys.

Here, intracranial volume (ICV) was statistically controlled to account for intersubject ICV differences, which are particularly large between males and females. Then, a permutation approach (Anderson and Robinson, 2001; Bullmore et al., 1999) using 10,000 iterations was used to calculate statistical inferences for all statistical analyses.

3. Results

3.1. Cortical surface modeling

Figure 1 shows three examples of cortical surface modeling results in three different subjects. The two surfaces are shown in red (GM-CSF) and blue (GM-WM) on three different views (panels (a) through (i)). The resulting cortical thickness maps for the three subjects as projected on the average cortical surface are shown in panels I–III. The average cortical surface itself is shown in Figure 2, labeled with major neuroanatomical landmarks (Table 2). It can be seen that the average cortical surface preserved the mor-
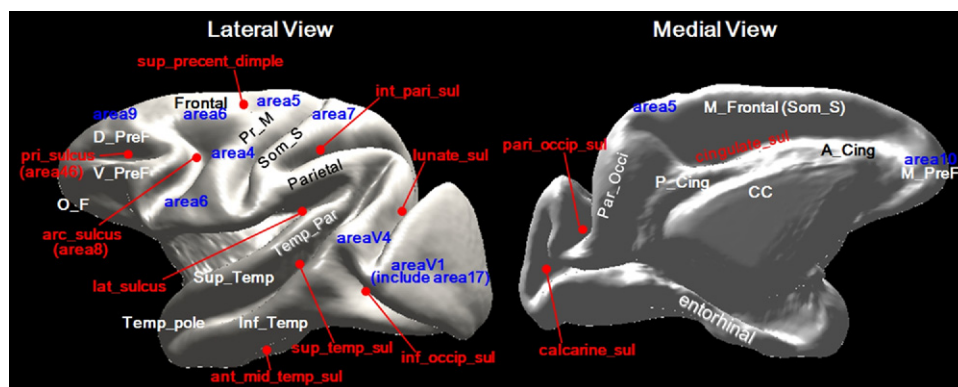

Fig. 2. Average Rhesus monkey brain surface. Left: lateral view of the left hemisphere. Right: medial view of the left hemisphere. Abbreviated anatomical terms are given as labels, and the abbreviation list is given in Table 2.

Table 2
Abbreviations used in Figure 2

Abbreviations	Full name
Sup-precent-dimple	superior precent dimple
pri-sulcus	principal sulcus
arc-sulcus	arcuate sulcus
lat-sulcus	lateral sulcus anterior midtemporal sulcus superior
ant-midtemp-sul	temporal sulcus inferior occipital sulcus
sup-temp-sul	lunate sulcus intraparietal sulcus
inf-occip-sul	cingulate sulcus parieto occipital sulcus
lunate-sul	calcarine sulcus
int-pari-sul	dorsal pefrontal
cingulate-sul	ventral prefrontal
pari-occip-sul	orbitofrontal
calcarine-sul	superior temporal
D-pref	inferior temporal
v-pref	temporal pole
O-f	temporo parietal
sup-Temp	parieto occipital
Inf-Temp	posterior cingulum medial frontal (somato-sensory)
Temp-pole	medial prefrontal corpus callosum
Temp-par	
Par-Occi	
P-cing	
M-frontal (Som-S)	
M-PreF	
CC	

phology of the major gyri and sulci of the individual surfaces.

3.2. Cortical thickness mapping—general characteristics

Local mean cortical thickness maps for the sex-matched groups of young and old monkeys were mapped onto the average surface (Figure 3a–b). Mean cortical thickness in the two different groups showed similar overall characteristics. The overall mean cortical thickness value for the whole group of monkeys was 2.37 ± 0.19 mm. The maximal cortical thickness was found in the frontal, medial-frontal, and temporal pole regions (3.55 ± 0.27 mm), whereas the minimal cortical thickness was found in the somato-sensory and occipital cortices (1.73 ± 0.16 mm).

3.3. Age-related effects on cortical thickness in monkeys

3.3.1. Group analyses

While mean cortical thickness across the whole cortex did not show statistically significant differences between the two age groups (2.31 ± 0.19 mm in the group of young monkeys and 2.35 ± 0.20 mm in the group of old monkeys), cortical thickness values for both age groups showed some significant age effects across manually defined regions of different lobes. These regional subdivisions are shown in Figure 4(i). Significant group differences were found in the right superior temporal lobe ($p < 0.01$, corrected), the left superior temporal lobe ($p < 0.05$, corrected) right cingulate cortex ($p < 0.05$ corrected) and the left cingulate cortex ($p < 0.01$ corrected). These findings are summarized in the bar graphs in Figure 4.

To more accurately assess the age effects between the two age groups, maps of group differences based on local vertex-wise analysis (*t*-test) were generated. Large clusters of statistically significant group differences were found between the two groups, and are shown in Figure 5. The largest *negative* age-related effects were found in the premotor (areas 4, 5) and somato-sensory cortices (area 7) ($p < 0.01$ corrected). Also, large clusters with *positive* age-related effects were found in the arcuate sulcus, the cingulate cortex, the temporo-parietal region, the superior temporal sulcus, and bilaterally in lateral junction of area V4 and V1. Significant positive age-related effects were also observed in the right temporal pole region and right dorsolateral prefrontal cortex, while smaller clusters with similar trends were also observed in the left hemisphere.

3.3.2. Linear regression analysis

Statistical maps (*p*-value) derived from the linear regression analysis between age and cortical thickness for the entire monkey group are shown in Figure 6. Significant negative age-related effects were found bilaterally in the pre- and post-central gyri in the premotor and somato-sensory cortices. Small clusters with positive age-related effects were found in the left cingulate cortex, the right arcuate sulcus, and in the right V1 and V4 areas.
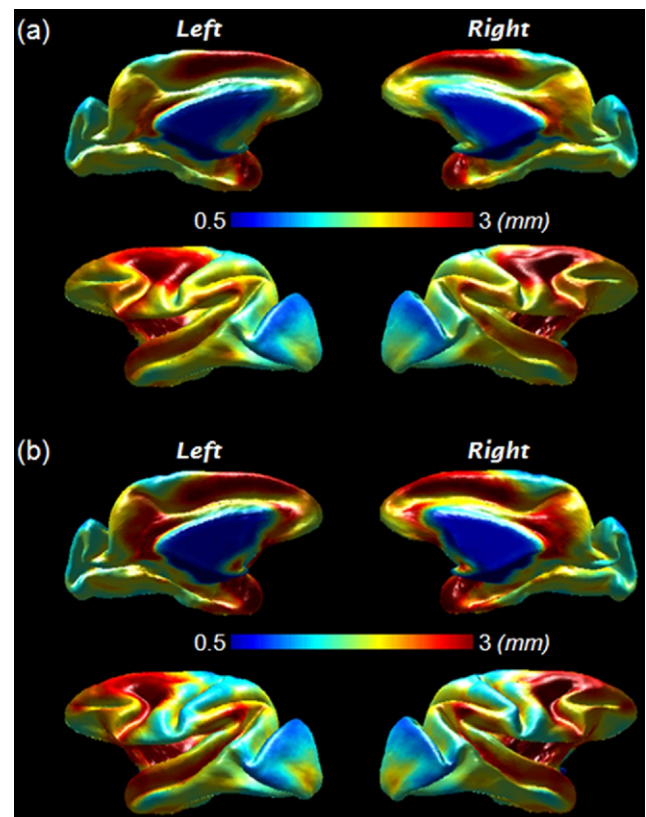

Fig. 3. Mean cortical thickness maps of the group of sex-matched young (a) and old monkeys (b).
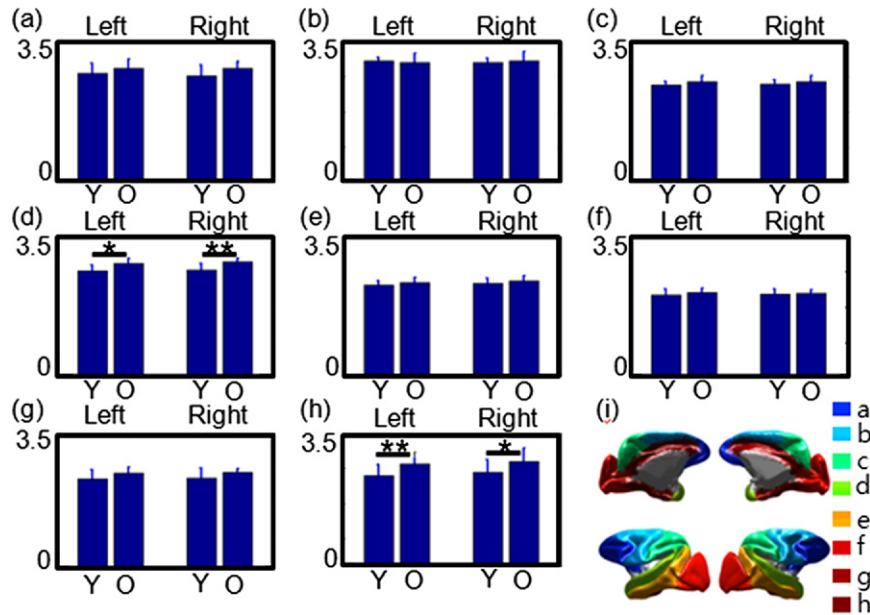
Fig. 4. Group regional mean cortical thickness analysis for the young and old age groups (left and right hemispheres are analyzed separately). The regional lobe-wise parcellation is given in panel (I), where a = prefrontal lobe, b = frontal lobe, c = parietal lobe, d = superior temporal lobe (temporal auditory cortex), e = inferior temporal lobe (temporal visual cortex), f = occipital lobe, g = temporal limbic region, h = cingulate cortex. In each bar graph: "Y"—young, "O"—old. Asterisk (∗) denotes statistically significant difference at significant level $p < 0.05$, and doubled asterisk (∗∗) denotes statistically significant difference at significant level $p < 0.01$.

4. Discussion

In this work, cortical thickness maps of 18 rhesus monkeys ranging in age from young (6.1 years) to very old (26.5 years) were calculated using optimized cortical surface modeling technique. Cortical thickness maps for all 18 monkeys were then tested for age-effects through vertex-wise linear regression analysis, and young-old partial grouping scheme for gender distribution matching was used for group comparisons.

Some of the regional age-related effects found in this work on the cortical thickness of the rhesus monkey have parallels in similar processes found in the human cortex, whereas other effects are either not replicated in humans or are opposite in trend. Our most robust finding here—age-related cortical thinning in the precentral and postcentral gyri—has been observed in several human studies (Salat et al., 2004; Sowell et al., 2003; Sowell et al., 2007). Some of
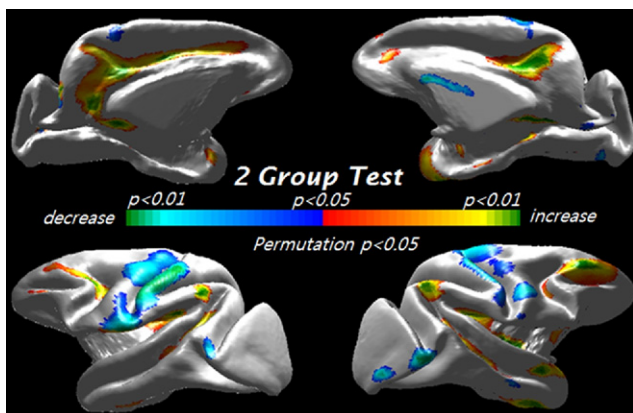

Fig. 5. Vertex-wise analysis of mean cortical thickness—group comparison between young and old monkeys. Upper panels—medial views of both hemispheres, lower panels—lateral views. Statistically significant differences (under random permutation based correction) are marked in color (green-blue: decrease/red-green: increase). The color bar is scaled to represent p-values between 0.01 and 0.05.
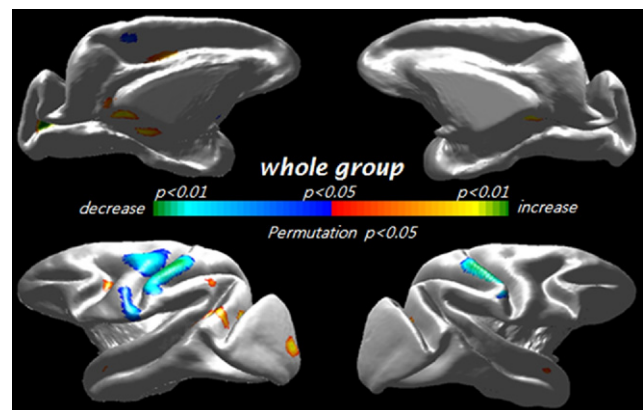

Fig. 6. Correlation analyses between cortical thickness and age for the entire group of monkeys in this study. Medial (upper row) and lateral (lower row) views of both hemispheres. Significant age-correlations (under random permutation based correction) are marked in colors. The color bar is scaled to represent p-values between $p < 0.05$ and $p < 0.01$. The blue scale denotes decrease and the red scale denotes increase in cortical thickness with age.

the less robust findings, such as the increase in cortical thickness in the cingulate cortex, the superior temporal sulcus, and near the principal sulcus (area 46) also correlate well with findings in humans (Salat et al., 2004; Ziegler et al., 2008).

The histological basis for age-related cortical thickness variations in the Rhesus monkey brain as well as in the human brain remains unclear. It has been previously shown that in the Rhesus monkey brain there is a thinning of cortical Layer 1 both in Brodmann area 46 in the prefrontal cortex (Peters et al., 1998) as well as in the visual cortex (Peters et al., 2001), a thinning that is not associated with loss in neurons, and is hypothesized to be more related to loss of dendritic arborization and loss of synaptic connections (Dickstein et al., 2007). The thinning observed in the pre- and postcentral gyri in this study and in previous studies in humans has yet to be understood on the histological level and is unlikely to be explained by the Layer 1 finding per se, because the amount of thinning histologically observed in the aforementioned studies is relatively minute, and seemingly has no effect on total cortical thickness (Peters and Sethares, 2002).

The increase in cortical thickness observed in, for instance, the cingulate gyrus, may reflect a loss of myelination in adjacent subcortical white matter, which then induces T_1 increases in that area and thus some "white matter pixels" on the gray/white matter border become clustered with gray matter in the segmentation process, creating the semblance of increased gray matter thickness. Age-related changes in gray/white matter contrast have been observed (Kochunov et al., 2008; Salat et al., 2009) and have been shown to have a potential effect on the determination of the gray/white matter interface, thus further histological validation is needed for a better understanding of this phenomenon.

Although the most simple and straightforward model for age-related effects on brain morphology is a linear correlation, this is by no means the most physiologically sound model. On the macroscopic level, studies have shown that given enough subjects, it is possible to detect nonlinear regional age-effects in gray matter volume (Sowell et al., 2003). Moreover, the pattern of those effects vary greatly from one region to the other, where in some regions the age effects occur at an earlier age, and in others the changes occur later in life. Similarly, changes in white matter volume may show increases in the early to middle age period, and then decline (Allen et al., 2005; Ge et al., 2002; Salat et al., 1999). The small population size of monkeys in this study prevented us from reliably performing such analysis. Moreover, the uneven distribution of males and females in our monkey population further prevented us from performing a three age-group analysis (young, middle-aged and old), which could have been used to as an alternative way to detect nonlinear age effects. It should also be noted that although we did try in this study to account for total brain volume and other sex effects, age-related patterns shown in

this study need to be carefully interpreted in view of the low number of subjects. A significantly larger number of subjects are needed for a statistically sound nonlinear analysis of such data, and it is hoped that with more monkeys scanned and with data sharing with other groups such analyses will become viable.

Notwithstanding the lack of basic understanding of its exact neurobiological significance, cortical thickness has been shown to correlate well with behavior in a host of other studies of various deficits (Dickerson et al., 2008; Narayan et al., 2007). Currently, what are missing are a full understanding of the relationship between cortical thickness and behavior on the one hand, and the link between cortical thickness and the underlying cortical microstructure on the other. Current opinions on the relationship between neuronal density, cortical surface characteristics and cortical density across the cortex and across species have shifted towards accepting that a large diversity of ratios exist between cortical thickness and neuronal density within the cortex of a specific species, and across species (Herculano-Houzel et al., 2008; Rakic, 2008). In this context, it is imperative for future studies to establish a connection between cortical thickness patterns of homologous functional areas in the human and monkey brains. Recent default network analysis showed significant resemblance between the network characteristics of the Rhesus monkey and the human brain (Vincent et al., 2007), where similarities were found in the posterior cingulate region and motor/somato-sensory area, while prefrontal region connectivity patterns were significantly different between the two species. In this study, similar age-related changes in cortical thickness patterns have been revealed in the motor/somato-sensory areas of both species, whereas cortical thickness in inferior-temporal and frontal/prefrontal regions seemed to have different age-related trajectories in humans and monkeys. Thus it is possible that in both species, age-related changes in cortical thickness are related to degradation of long-range white matter connections. Such relationship between cortical properties and long-range connections has been proposed (Zhang and Sejnowski, 2000), but this link needs to be further corroborated in more functional, connectivity and histological studies.

5. Conclusions

Robust age-related effects on cortical thickness of the rhesus monkey brain were reported with significant age-related cortical thinning in the precentral and postcentral gyri, as well as increases in cortical thickness in the superior temporal sulcus, the temporal pole and in the anterior cingulate cortex. These results emphasize the utility of the monkey model as a highly controlled model for normal aging, and call for further independent corroboration as well as detailed investigation of the histological basis in the areas

that show robust age-related effects as well as the behavioral correlates to these changes.

Acknowledgments

References

Alexander, G.E., Chen, K., Aschenbrenner, M., Merkley, T.L., Santerre-Lemmon, L.E., Shamy, J.L., Skaggs, W.E., Buonocore, M.H., Rapp, P.R., Barnes, C.A., 2008. Age-related regional network of magnetic resonance imaging gray matter in the rhesus macaque. J. Neurosci. 28, 2710–2718.

Allen, J.S., Bruss, J., Brown, C.K., Damasio, H., 2005. Normal neuroanatomical variation due to age: The major lobes and a parcellation of the temporal region. Neurobiol. Aging 26, 1245–1260.

Anderson, M.J., Robinson, J., 2001. Permutation tests for linear models. Aust. N Z J. Stat. 43, 75–88.

Bullmore, E.T., Suckling, J., Overmeyer, S., Rabe-Hesketh, S., Taylor, E., Brammer, M.J., 1999. Global, voxel, and cluster tests, by theory and permutation, for a difference between two groups of structural MR images of the brain. IEEE Trans. Med. Imaging 18, 32–42.

Cocosco, C.A., Zijdenbos, A.P., Evans, A.C., 2003. A fully automatic and robust brain MRI tissue classification method. Med. Image Anal. 7, 513–527.

Collins, D.L., Neelin, P., Peters, T.M., Evans, A.C., 1994. Automatic 3D intersubject registration of MR volumetric data in standardized Talairach space. J. Comput. Assist. Tomogr. 18, 192–205.

Dale, A.M., Fischl, B., Sereno, M.I., 1999. Cortical surface-based analysis. I. Segmentation and surface reconstruction. Neuroimage 9, 179–194.

Dickerson, B.C., Fenstermacher, E., Salat, D.H., Wolk, D.A., Maguire, R.P., Desikan, R., Pacheco, J., Quinn, B.T., Van der Kouwe, A., Greve, D.N., Blacker, D., Albert, M.S., Killiany, R.J., Fischl, B., 2008. Detection of cortical thickness correlates of cognitive performance: Reliability across MRI scan sessions, scanners, and field strengths. Neuroimage 39, 10–18.

Dickstein, D.L., Kabaso, D., Rocher, A.B., Luebke, J.I., Wearne, S.L., Hof, P.R., 2007. Changes in the structural complexity of the aged brain. Aging Cell 6, 275–284.

Fischl, B., Dale, A.M., 2000. Measuring the thickness of the human cerebral cortex from magnetic resonance images. Proc. Natl. Acad. Sci. USA 97, 11050–11055.

Fjell, A.M., Walhovd, K.B., Reinvang, I., Lundervold, A., Salat, D., Quinn, B.T., Fischl, B., Dale, A.M., 2006. Selective increase of cortical thickness in high-performing elderly − structural indices of optimal cognitive aging. Neuroimage 29, 984–994.

Franklin, M.S., Kraemer, G.W., Shelton, S.E., Baker, E., Kalin, N.H., Uno, H., 2000. Gender differences in brain volume and size of corpus callosum and amygdala of rhesus monkey measured from MRI images. Brain Res. 852, 263–267.

Ge, Y., Grossman, R.I., Babb, J.S., Rabin, M.L., Mannon, L.J., Kolson, D.L., 2002. Age-related total gray matter and white matter changes in normal adult brain. Part I: volumetric MR imaging analysis. AJNR Am. J. Neuroradiol. 23, 1327–1333.

Herculano-Houzel, S., Collins, C.E., Wong, P., Kaas, J.H., Lent, R., 2008. The basic nonuniformity of the cerebral cortex. Proc. Natl. Acad. Sci. U S A 105, 12593–12598.

Herndon, J.G., Moss, M.B., Rosene, D.L., Killiany, R.J., 1997. Patterns of cognitive decline in aged rhesus monkeys. Behav. Brain Res. 87, 25–34.

Jernigan, T.L., Archibald, S.L., Fennema-Notestine, C., Gamst, A.C., Stout, J.C., Bonner, J., Hesselink, J.R., 2001. Effects of age on tissues and regions of the cerebrum and cerebellum. Neurobiol. Aging 22, 581–594.

Kim, J.S., Singh, V., Lee, J.K., Lerch, J., Ad-Dab'Bagh, Y., MacDonald, D., Lee, J.M., Kim, S.I., Evans, A.C., 2005. Automated 3-D extraction and evaluation of the inner and outer cortical surfaces using a Laplacian map and partial volume effect classification. Neuroimage 27, 210–221.

Kochunov, P., Thompson, P.M., Coyle, T.R., Lancaster, J.L., Kochunov, V., Royall, D., Mangin, J.F., Riviere, D., Fox, P.T., 2008. Relationship among neuroimaging indices of cerebral health during normal aging. Hum Brain Mapp 29, 36–45.

Lee, J., Lee, J.M., Kim, J.H., Kim, I.Y., Evans, A.C., Kim, S.I., 2006. A novel quantitative validation of the cortical surface reconstruction algorithm using MRI phantom: issues on local geometric accuracy and cortical thickness. In: Medical Image Computing and Computer-Assisted Intervention: MICCAI International Conference on Medical Image Computing and Computer-Assisted Intervention 9, (Pt 1), p. 183–190.

Lerch, J.P., Evans, A.C., 2005. Cortical thickness analysis examined through power analysis and a population simulation. Neuroimage 24, 163–173.

Lyttelton, O., Boucher, M., Robbins, S., Evans, A., 2007. An unbiased iterative group registration template for cortical surface analysis. Neuroimage 34, 1535–1544.

Matochik, J.A., Chefer, S.I., Lane, M.A., Woolf, R.I., Morris, E.D., Ingram, D.K., Roth, G.S., London, E.D., 2000. Age-related decline in striatal volume in monkeys as measured by magnetic resonance imaging. Neurobiol. Aging 21, 591–598.

McLaren, D.G., Kosmatka, K.J., Oakes, T.R., Kroenke, C.D., Kohama, S.G., Matochik, J.A., Ingram, D.K., Johnson, S.C., 2009. A population-average MRI-based atlas collection of the rhesus macaque. Neuroimage 45, 52–59.

Moss, M.B., Killiany, R.J., Lai, Z.C., Rosene, D.L., Herndon, J.G., 1997. Recognition memory span in rhesus monkeys of advanced age. Neurobiol. Aging 18, 13–19.

Moss, M.B., Rosene, D.L., Peters, A., 1988. Effects of aging on visual recognition memory in the rhesus monkey. Neurobiol. Aging 9, 495–502.

Narayan, V.M., Narr, K.L., Kumari, V., Woods, R.P., Thompson, P.M., Toga, A.W., Sharma, T., 2007. Regional cortical thinning in subjects with violent antisocial personality disorder or schizophrenia. Am. J. Psychiatry 164, 1418–1427.

Peters, A., Moss, M.B., Sethares, C., 2001. The effects of aging on layer 1 of primary visual cortex in the rhesus monkey. Cereb. Cortex 11, 93–103.

Peters, A., Sethares, C., 2002. The effects of age on the cells in layer 1 of primate cerebral cortex. Cereb. Cortex 12, 27–36.

Peters, A., Sethares, C., Moss, M.B., 1998. The effects of aging on layer 1 in area 46 of prefrontal cortex in the rhesus monkey. Cereb. Cortex 8, 671–684.

Rakic, P., 2008. Confusing cortical columns. Proc. Natl. Acad. Sci. U S A 105, 12099–12100.

Raz, N., Lindenberger, U., Rodrigue, K.M., Kennedy, K.M., Head, D., Williamson, A., Dahle, C., Gerstorf, D., Acker, J.D., 2005. Regional brain changes in aging healthy adults: general trends, individual differences and modifiers. Cereb. Cortex 15, 1676–1689.

Raz, N., Rodrigue, K.M., 2006. Differential aging of the brain: patterns, cognitive correlates and modifiers. Neurosci. Biobehav. Rev. 30, 730–748.

Robbins, S., Evans, A.C., Collins, D.L., Whitesides, S., 2004. Tuning and comparing spatial normalization methods. Med. Image Anal. 8, 311–323.

Roth, G.S., Mattison, J.A., Ottinger, M.A., Chachich, M.E., Lane, M.A., Ingram, D.K., 2004. Aging in rhesus monkeys: relevance to human health interventions. Science 305, 1423–1426.

Salat, D.H., Buckner, R.L., Snyder, A.Z., Greve, D.N., Desikan, R.S., Busa, E., Morris, J.C., Dale, A.M., Fischl, B., 2004. Thinning of the cerebral cortex in aging. Cereb. Cortex 14, 721–730.

Salat, D.H., Kaye, J.A., Janowsky, J.S., 1999. Prefrontal gray and white matter volumes in healthy aging and Alzheimer disease. Arch. Neurol. 56, 338–344.

Salat, D.H., Lee, S.Y., van der Kouwe, A.J., Greve, D.N., Fischl, B., Rosas, H.D., 2009. Age-associated alterations in cortical gray and white matter signal intensity and gray to white matter contrast. Neuroimage 48, 21–28.

Sled, J.G., Zijdenbos, A.P., Evans, A.C., 1998. A nonparametric method for automatic correction of intensity nonuniformity in MRI data. IEEE Trans. Med. Imaging 17, 87–97.

Smith, S.M., 2002. Fast robust automated brain extraction. Hum. Brain Mapp. 17, 143–155.

Sowell, E.R., Peterson, B.S., Kan, E., Woods, R.P., Yoshii, J., 2007. Sex Differences in Cortical Thickness Mapped in 176 Healthy Individuals between 7 and 87 Years of age. Cereb. Cortex 17, 1550–1560.

Sowell, E.R., Peterson, B.S., Thompson, P.M., Welcome, S.E., Henkenius, A.L., Toga, A.W., 2003. Mapping cortical change across the human life span. Nat. Neurosci. 6, 309–315.

Styner, M., Knickmeyer, R., Joshi, S., Coe, C., Short, S.J., 2007. Automatic Brain Segmentation in Rhesus Monkeys. Proceedings of the SPIE Medical Imaging, 65,122 L1-8.

Tigges, J., Gordon, T.P., McClure, H.M., Hall, E.C., Peters, A., 1988. Survival rate and life span of rhesus monkeys at the Yerkes regional primate Research Center. Am. J. Primatol. 15, 263–273.

Van Essen, D.C., Lewis, J.W., Drury, H.A., Hadjikhani, N., Tootell, R.B., Bakircioglu, M., Miller, M.I., 2001. Mapping visual cortex in monkeys and humans using surface-based atlases. Vis. Res. 41, 1359–1378.

Vincent, J.L., Patel, G.H., Fox, M.D., Snyder, A.Z., Baker, J.T., 2007. Intrinsic functional architecture in the anaesthetized monkey brain. Nature 447, 83–86.

Walhovd, K.B., Westlye, L.T., Amlien, I., Espeseth, T., Reinvang, I., Raz, N., Agartz, I., Salat, D.H., Greve, D.N., Fischl, B., Dale, A.M., Fjell, A.M., 2009. Consistent neuroanatomical age-related volume differences across multiple samples. Neurobiol. Aging. June 29 [Epub ahead of print].

Wisco, J.J., Killiany, R.J., Guttmann, C.R., Warfield, S.K., Moss, M.B., Rosene, D.L., 2008. An MRI study of age-related white and gray matter volume changes in the rhesus monkey. Neurobiol. Aging 29, 1563–1575.

Zhang, K., Sejnowski, T.J., 2000. A universal scaling law between gray matter and white matter of cerebral cortex. Proc. Natl. Acad. Sci. U S A 97, 5621–5626.

Ziegler, D.A., Piguet, O., Salat, D.H., Prince, K., Connally, E., Corkin, S., 2008. Cognition in healthy aging is related to regional white matter integrity, but not cortical thickness. Neurobiol. Aging. Dec 15 [Epub ahead of print].